

## Section 3

# PROGRESS IN BIOPHYSICAL RESEARCH

### 3.A Application of Nanosecond X-Ray Diffraction Techniques to Bacteriorhodopsin

The use of x-ray diffraction methods to investigate atomic structures in biological macro molecules has been common for many years<sup>11</sup>. In the past, because of the long exposure times needed for good quality records, the measurements have almost all been of static subjects. With the advent of intense x-ray sources from laser produced plasmas, it becomes possible to make x-ray diffraction measurements with sub nanosecond exposures. As an illustration, we are preparing to adopt x-ray diffraction techniques to study the photo response of bacteriorhodopsin in purple membrane.

The bacteriorhodopsin (BR) in the purple membrane (PM) of the halobacterium halobium has been clearly demonstrated to be a light activated photon pump<sup>12</sup>. One particular issue under debate involves the magnitude of any conformational change that may take place during the BR photocycle. We hope to contribute to the resolution of this question by using the newly developed laser plasma x-ray source<sup>13</sup> to obtain subnanosecond x-ray diffraction patterns throughout the course of the 20 millisecond photocycle.

The x-ray diffraction patterns discussed above require approximately  $10^{10}$  photons of nearly monochromatic light. It has been demonstrated in many laboratories that laser produced plasmas are reasonably efficient producers of soft x-ray radiation. With the proper choice of target materials and laser intensity, a large part of the x-ray radiation may be channelled into a few narrow emission lines<sup>14</sup>. For x-ray diffraction studies, x-ray sources in the 4.5 Å - 1.5 Å region of the spectrum with a spectral spread of less than 1% are appropriate.

To generate the purple membrane diffraction pattern discussed below, the single beam Nd<sup>+3</sup> Glass Development Laser at the University of Rochester's Laboratory for Laser Energetics (LLE)<sup>15</sup> was used. This laser delivers single pulses of 1.054 μm light with full width at half maximum that can be varied from 50 - 700 psec. With newly added active mirror booster amplifiers<sup>16</sup> peak pulse powers of greater than 1 TW have been obtained with short pulses and a maximum energy of 250 joule with long pulses. The laser output aperture was 15 cm. Our system repetition rate was 2 pulses/hour.

Laser pulses were brought to a focus of 100 μm in a 24 inch diameter vessel which was evacuated to  $1 \times 10^{-5}$  Torr. Plasmas must be produced in a vacuum to prevent air breakdown before the laser light reaches the surface of the target.

Attached to the target chamber was an x-ray camera (shown in Figure 13) consisting of a nickel coated grazing reflection toroidal mirror<sup>17</sup> with a focal length of 62.5 cm and a mean angle of incidence of 0.91 degrees. The collection solid angle of the collector was  $2.4 \times 10^{-4}$  steradians. The system also included an annular aperture in the reflected x-ray beam, a controlled environment sample chamber, a controlled environment sample chamber, an annular aperture in the reflected x-ray beam, a controlled environment sample chamber,

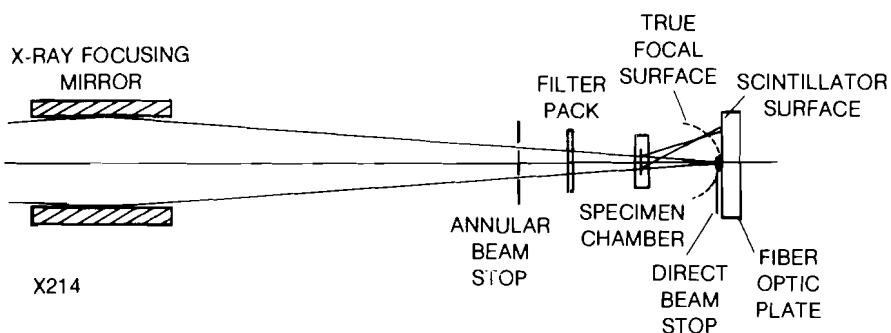


Figure 13 Schematic diagram of x-ray diffraction camera. The true focal surface of the camera is a sphere tangent to the sample and also tangent to the flat phosphor plane.

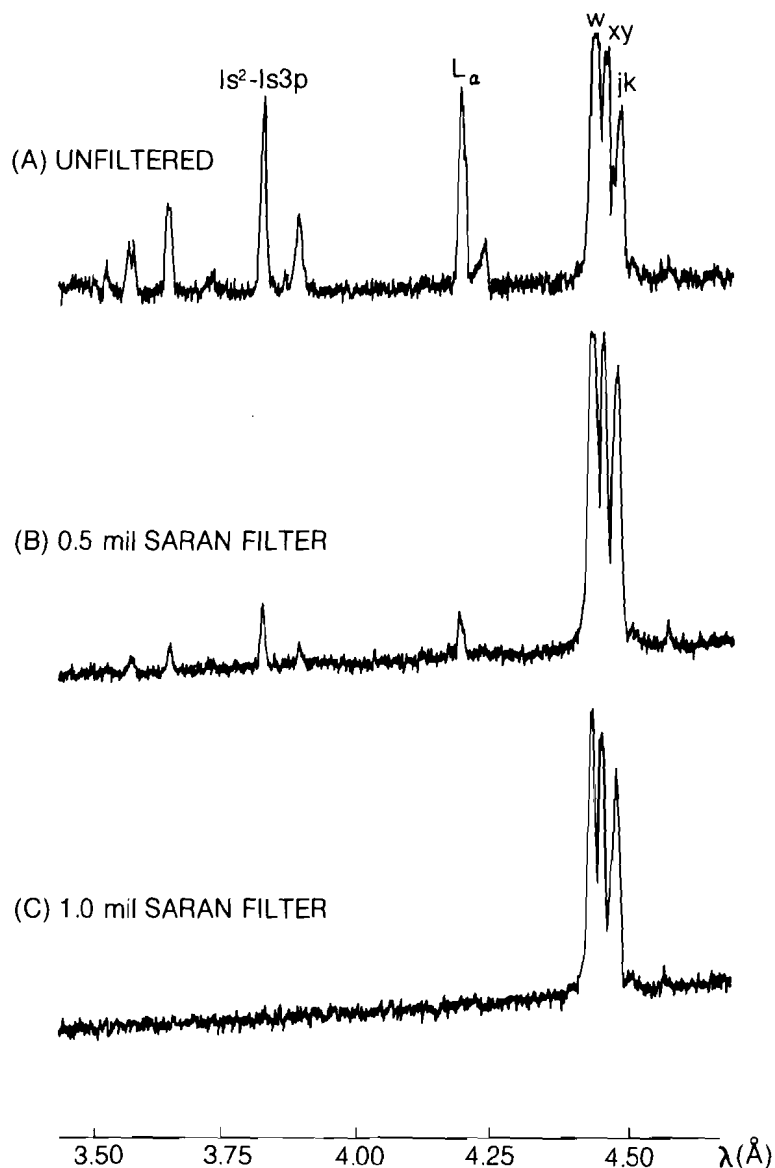
and a scintillator-image intensifier recording system. The 40 mm ZnS (Ag) scintillator was located 125 cm from the laser plasma source and was coupled to an Amperex model XX1360 25 mm channel plate intensifier through a fiberoptic faceplate. The intensifier had an adjustable luminosity gain of up to  $7 \times 10^4$  and was housed in a mount permitting direct attachment of various 35 mm and Polaroid camera backs. A lead disc 2.5 mm in diameter was mounted just in front of the scintillator plane to block the direct beam from the x-ray mirror.

Our experiments so far have been performed with highly chlorinated targets; room temperature saran ( $C_2H_2Cl_2$ ) and pressed polycrystals of hexachloroethane ( $C_2Cl_6$ ) held at 77°K (low temperature inhibits hexachloroethane sublimation in the vacuum chamber) have been used. In a saran plasma produced by irradiation with an incident 175J, 700 psec laser pulse focussed to  $\sim 10^{15}$  watts/cm<sup>2</sup>, about  $5 \times 10^{-4}$  of the incident laser energy (or  $\sim 3 \times 10^{14}$  photons) is radiated by  $Cl^{+15}$  at 4.45 Å in a wavelength interval of  $\Delta\lambda/\lambda$  of  $8 \times 10^{-3}$ . Since x-ray production by plasma ions is proportional to the ion density, the hexachloroethane produces about twice the x-ray flux of saran. For simplicity, however, saran was the target used in most test shots.

A typical emission spectrum from a saran plasma is shown in Figure 14a. In addition to the intense line radiation at 4.45 Å we have x-ray lines at shorter wavelengths and a much weaker background continuum. Effective monochromatization of this emission is possible by means of thin saran foils. Such filtered spectra are shown in Figures 14b and 14c corresponding to 12.5 μm and 25 μm foil thicknesses, respectively. The 25 μm foil transmits 57% of the desired line radiation. Outside the spectral range shown in Figure 14 we filter the long wavelength components with a 25 μm beryllium foil while the short wavelength radiation is not reflected by the toroidal mirror.

Figure 15 shows an x-ray powder diffraction pattern from a PM stack recorded on 2475 high speed recording film. It was obtained with a single 700 psec 220 joule pulse focussed on an hexachloroethane target; the camera collected  $\sim 3-4 \times 10^9$  photons for diffraction. The identifiable reflections are noted. The diffraction rings are indexed on a 2-dimensional P-3 hexagonal lattice<sup>18</sup>. Typical high quality PM powder patterns have been obtained using rotating

Figure 14 Chlorine spectra from saran targets on three different laser shots showing the effect of saran filtration. All shots were approximately 170 J in 700 psec. The  $Cl^{+15}$  resonance line (w) and its associated satellites (x, y, j, k) are the components useful for x-ray diffraction. The  $1s^2-1s3p$  is a higher energy  $Cl^{+15}$  emission line. The  $L\alpha$  is radiated from  $Cl^{+16}$  ions. Filtration for (A) was 25  $\mu m$  Be; for (b) 25  $\mu m$  + 12/5  $\mu m$  saran; for (c) 25  $\mu m$  saran. In (C) the transmission of the resonance line and its satellites was 57% while all other lines were almost completely absorbed.



X216

anode tube sources and exposure times of 20 - 50 hours<sup>19,20</sup>. In these patterns strong rings out to 7 Å resolution are observed, while weaker rings out to 3.5 Å are also seen. In our pattern the lower resolution orders are well resolved and quite intense. They extend out to a resolution of ~ 15 Å and are good enough for quantitative data reduction and structure determination. The high resolution orders, although intrinsically as bright as the lower orders are out of focus in Figure 15. This is primarily because the scintillator used in this experiment was deposited on a flat fiber optic surface. The actual focal surface of the x-ray camera is a sphere tangent to the sample and to the mirror focus<sup>17</sup> as shown in Figure 13.

In a time resolved experiment, a master timing signal will generate an electrical pulse, and initiate a green laser stimulus pulse to a hydrated purple membrane stack situated in the humid sample chamber of the x-ray camera. Then, after a delay ranging from nanoseconds to tens of milliseconds, the main laser will fire, generating plasma-produced x-rays which will yield an x-ray diffraction pattern. By varying the delay, a stroboscopic series of diffraction patterns will be obtained.

The information contained in these powder patterns can be used along with the phase information obtained from electron diffraction studies to yield a two dimensional projection of the electron density of the purple membrane perpendicular to the plane of the membrane. This view offers a great deal of information about the bacteriorhodopsin (BR) because the seven helices of the BR are arrayed roughly perpendicular to the membrane plane. That is, the projection looks down the helical chains. Hence, for example, in a dynamic experiment conformational changes involving movement of the helices may be readily apparent.

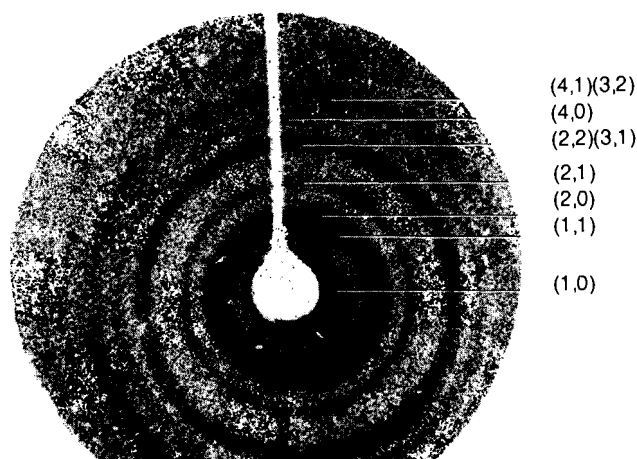


Figure 15 *Purple membrane diffraction pattern. The sample-phosphor separation was 2.7 cm. Identified are rings indexed on a hexagonal lattice. Higher resolution rings are out of focus due to spherical focal plane of the camera.*

LASER PULSE ENERGY - 213 Joules    X-RAY SOURCE -  $\text{Cl}^{+15}$  LASER HEATED PLASMA  
 LASER PULSE WIDTH - 700 psec    X-RAY WAVELENGTH - 4.45 Å

X209